Dissociation of H$_2$ on Cu(100): Dynamics on a new two-dimensional potential energy surface

G. Wiesenekker, G. J. Kroes, and E. J. Baerends

Theoretische Chemie, Vrije Universiteit, De Boelelaan 1083, 1081 HV Amsterdam, The Netherlands

R. C. Mowrey

Chemistry Division, Naval Research Laboratory, Washington, DC 20375-5342

A two-dimensional (2-D) potential energy surface (PES) has been calculated for H$_2$ interacting with the (100) face of copper. The PES is for H$_2$ approaching with its internuclear axis parallel to the surface and dissociating over a bridge site into neighboring hollow sites. The density functional calculations were performed both within the local density approximation (LDA) and within a generalized gradient approximation (GGA). The LDA surface shows no barrier to chemisorption, but the GGA surface has a barrier of height 0.4 eV. A fit of the GGA surface has been used to calculate reaction probabilities for H$_2$ in its $v=0$ and $v=1$ vibrational states, employing a wave packet method. The 2-D wave packet results for the $v=0$ and $v=1$ thresholds are consistent with experiment, indicating that the barrier height calculated within the GGA used is accurate. The GGA results for the value of the barrier height are also consistent with the GGA value (0.5 eV) recently obtained for H$_2$+Cu(111) by Hammer *et al.* [Phys. Rev. Lett. **73**, 1400 (1994)], but the GGA value recently computed for H$_2$+Cu(100) (0.9 eV) by White *et al.* is too high [Phys. Rev. Lett. **73**, 1404 (1994)]. © *1995 American Institute of Physics.*

I. INTRODUCTION

The dissociation of molecular hydrogen on copper surfaces has become a standard model for the direct dissociative chemisorption of H$_2$ on a metal surface. Work done on the H$_2$+Cu system and aimed at calculating the "threshold" or "barrier" to the reaction includes experiments,[1-11] electronic structure calculations,[12-19] and dynamical studies.[20-39] The experimentally obtained reaction probabilities or sticking coefficients can be interpreted in terms of reaction thresholds, which are related to the barrier height obtained from electronic structure studies in a nontrivial way.[33,36] Tested against experiment, dynamics studies are the ultimate test of the accuracy of proposed potential energy surfaces (PES's), in addition to being helpful in interpreting the experimental findings. Much work has been done to understand the mechanism of the dissociation and to investigate the effects of molecular vibration[33,36] and rotation.[28,39,40]

A recent careful investigation[41] of available experimental results has put the threshold to dissociation for H$_2$ in its ground vibrational state at approximately 0.5 eV. The barrier height accessible through electronic structure calculations should then be of roughly the same size. Obviously, in calculating the barrier height care must be taken that the errors (either in the theoretical model or in the numerical methods used to solve the theoretical model) are not of the same order as the barrier itself. The required accuracy has only recently become available[12,19,42,43] from density functional calculations using gradient corrections in conjunction with the use of slabs to model the interaction of the molecule with the metal.

In this work, we use density functional theory (DFT) within the local density approximation (LDA) and within a generalized gradient approximation (GGA) to obtain a two-dimensional (2-D) potential energy surface for H$_2$ interacting with Cu(100). Studies on molecular systems have shown that the binding energies calculated using the LDA are usually too large, and that GGA's correct for this overbinding.[44-48] A recent study arrived at a similar conclusion for the molecular chemisorption of CO on Cu(100).[43] Other recent work on dissociative chemisorption of H$_2$ on Al(110) (Refs. 42 and 49), Cu(111) (Ref. 12), and Cu(100) (Ref. 19) has shown that the barrier heights calculated using the LDA are too low.

In the DFT calculations we present, the interaction of H$_2$ with Cu(100) is modeled using a laterally infinite slab containing a finite number of layers of Cu atoms and interacting with a periodic overlayer of H$_2$. The slab geometry is expected to give a good description of the metallic properties of the surface, and calculations on CO+Cu(100) have shown good convergence of the chemisorption energy with size of the unit cell (coverage) and the number of layers used in the slab.[43,50] While cluster calculations can yield useful qualitative insights concerning the PES, a problem with cluster calculations is that the chemisorption energy converges poorly with cluster size.[50,51]

Our present purpose is twofold. First, we check our DFT results for consistency with the experimental results. For this purpose, an accurate fit of the GGA surface is made. The fit is then used to calculate reaction thresholds for H$_2$ in its $v=0$ and $v=1$ vibrational states employing a 2-D wave packet method.[52] It is now known[25-27,30,38,53] that for an accurate calculation of the thresholds it should be necessary to take into account all the molecular degrees of freedom, necessitating a 6-D dynamics study on a 6-D PES. However, it is also known that the error in the 2-D results is systematic, in that the 2-D thresholds calculated for the molecule dissociating in a favorable orientation and on a favorable site are

usually too low by 0.1–0.2 eV.[27,38,53] We can then use this knowledge in combination with the results from the 2-D wave packet calculations to arrive at a preliminary assessment of the accuracy of the calculated GGA barrier. We hope to extend our PES to higher dimensions and perform higher dimensionality dynamics calculations in the future.

Second, we check our DFT results for consistency with other recent GGA-slab results for the same system[19] and also for H_2+Cu(111).[12] Such checks should be useful for several reasons. In slab calculations, where we have to also consider convergence with the size of the unit cell and the number of layers in the slab, we are at present far from the situation that exists for calculations on small molecules, where benchmark DFT[45] and *ab initio* results are available to much higher accuracy. At the same time, small implementation errors can easily result in errors in the barrier height of a few tenths of an eV.[18,19] In such a situation it is obviously of use to compare results of using slightly different methods for identical or similar systems.

In Sec. II, we give a short description of the BAND program used to calculate the PES's. We also give results of convergence tests and present the results of the DFT calculations in this section, comparing our results with those of others for the H_2+Cu system. Section III gives an account of the procedure used to fit the GGA surface. The wave packet method used to calculate reaction thresholds is presented in Sec. IV. In this section we also present the results of the dynamics calculations and compare with experiment. Section V gives our conclusions.

II. ELECTRONIC STRUCTURE CALCULATIONS

A. Density functional method

The PES's discussed in this work were calculated using BAND,[54] which is a program for solving the Kohn–Sham equations[55,56] for periodic systems. In calculations employing periodicity in two directions using BAND, the one-electron states can be expanded in flexible basis sets consisting of numerical atomic orbitals (NAO's), Slater-type orbitals (STO's), or a combination of both. The core electrons of heavier atoms can be modeled using the frozen core approximation, avoiding the need for using pseudopotentials. In BAND, the matrix elements of the Hamiltonian are calculated using an accurate Gauss-type numerical integration scheme.[57] The **k**-space integration can be done accurately using the quadratic tetrahedron method.[58] No shape approximations are made to the potentials. The error in the binding energy as a result of the numerical methods used in BAND to solve the Kohn–Sham equations, such as the integrations in real space and in **k** space, are well below the errors in the binding energy due to intrinsic errors such as the choice of basis set, the size of the unit cell or coverage (to approximate single-molecule adsorption), and the number of layers in the slab, to be discussed below.

In a LDA calculation, the exchange-correlation energy is calculated using the Vosko–Wilk–Nusair (VWN) formulas.[59] Recently, gradient corrections have also been implemented in the program. In a GGA calculation, we use the Becke correction[60] for the exchange energy and the Perdew

correction[61] for the correlation energy. The gradient corrections for the total energy are calculated from the self-consistent LDA densities. Other calculations have shown this to be an excellent approximation to the binding energy calculated from the self-consistent nonlocal density.[12]

B. Convergence

The accuracy of the binding energies as calculated by BAND depends on the basis sets, the coverage to approximate the single atom/molecule adsorption, the number of layers in the slab to approximate the semi-infinite slab, and the accuracy of the numerical integration schemes used. We will address each of these points in some detail.

Basis sets. The basis sets for H and Cu consisted of a numerical atomic orbital and a Slater-type orbital, supplemented by polarization functions (abbreviated as NAO +STO+P in the tables below). The details of the basis set can be found in Table I. As the basis sets used are somewhat unconventional, we have calculated the equilibrium distances, dissociation energies, and lowest vibrational frequencies of the H_2 and CuH molecules with these basis sets and also with standard triple zeta basis sets with polarization functions (abbreviated as TZ+P in the tables below). The VWN functional[59] with the gradient corrections of Becke[60] and Perdew[62] have been used here as in all the results of the convergence tests presented below. The Cu atoms have a frozen core up to $3p$. For H_2 we can also compare the results to the basis set free result as calculated by Becke with the NUMOL program.[63] The results are given in Tables II and III. We see that the NAO+STO+P basis sets give almost the same results as the TZ+P basis sets. Comparing the results of using the NAO+STO+P basis set with the results of the basis set free calculations for H_2,[63] we also find good convergence with respect to the size of the basis set used for H_2.

TABLE I. The character and the exponent of the Slater functions for the basis sets for the H and Cu atoms. NAO is a numerical atomic orbital, obtained from a Herman–Skilmann-type calculation.

H	Cu $3p$ core	Cu $3d$ core
$1s$ NAO	$3d$ NAO	$4s$ NAO
$1s$ 1.58	$3d$ 1.65	$4s$ 1.0
$2s$ 1.0	$4s$ NAO	
$2p$ 1.0	$4s$ 1.0	
	$4p$ 2.0	

TABLE II. Properties of the free H_2 molecule as calculated with a basis set consisting of a numerical atomic orbital, a Slater-type orbital, and a polarization function (NAO+STO+P) or with a basis set consisting of three Slater-type orbitals and polarization functions (TZ+P). NUM is the basis set free result.

H_2	NAO+STO+P	TZ+P	NUM	Expt.
Bond length (Å)	0.75	0.75	0.75	0.74
Dissociation energy (eV)	4.81	4.83	4.9	4.8
Vibration freq. (cm⁻¹)	4304	4315	4330	4400

TABLE III. Properties of the free CuH molecule as calculated with a basis set consisting of a numerical atomic orbital, a Slater-type orbital, and a polarization function (NAO+STO+P) or with a basis set consisting of three Slater-type orbitals and polarization functions (TZ+P).

CuH	NAO+STO+ P	TZ+P	Expt.
Bond length (Å)	1.48	1.48	1.46
Dissociation energy (eV)	2.84	2.82	2.89
Vibration freq. (cm^{-1})	1926	1900	1940

Coverage. In calculating the energy of H_2 interacting with a Cu surface, we approximate the interaction energy in the zero coverage limit by calculating the interaction energy of a periodic overlayer of hydrogen molecules adsorbed to a copper slab. Obviously the coverage has to be small enough to ensure that direct or indirect (through-lattice) interactions between neighboring molecules are negligible. In the calculation of the PES's presented below we have used a (2×2) overlayer of hydrogen molecules [see Fig. 1 for a schematic plot of the (2×2) overlayer of H_2 located at bridge sites on a Cu (100) surface]. The copper slab is set up using the experimental lattice constant of 4.822 bohrs. To assess the importance of the direct interactions between the hydrogen molecules in the overlayer, we plot in Fig. 2, for different values of the hydrogen–hydrogen intramolecular distance r, the difference between the energy of a bare (2×2) overlayer of H_2
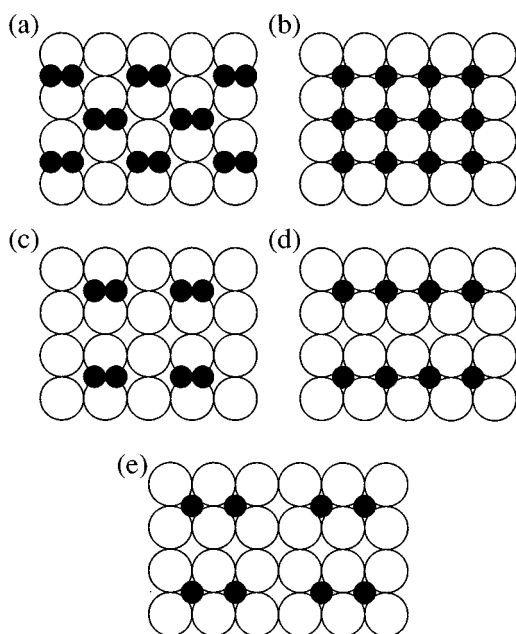

FIG. 2. The difference between the energy per unit cell of the bare 2×2 H_2 overlayer and the energy of a free H_2 molecule is plotted as a function of the internuclear distance between the H atoms. In the overlayer calculation, the centers of mass of the molecules are placed on sites corresponding to bridge sites of Cu(100), dissociation taking place into neighboring hollow sites.

molecules (i.e., the energy per unit cell containing one H_2 molecule) with the energy of a free hydrogen molecule. As can be seen, the direct interaction between neighboring hydrogen molecules is negligible for bond distances $\leqslant 4$ bohrs and in particular also for distances near the saddle point in the PES (approximately 2 bohrs, see below). The differences observed at bond distances larger than 4 bohrs are due to the distances between H atoms of different, neighboring molecules becoming similar to the H_2 bond length (for $r = 4.8$ bohrs, a 2×1 overlayer of H atoms absorbed in the hollow sites is obtained, and the H–H distance between atoms of neighboring molecules also becomes 4.8 bohrs, see Fig. 1). At these bond distances, contacts between H atoms of neighboring H_2 molecules lower the energy by 0.1–0.2 eV, which is of the same order as the H_2 bond energy at $r = 4.8$ a_0. Thus our calculated PES's could well be in error by 0.1–0.2 eV for $r > 4$ bohrs, but these errors should not affect the calculation of the reaction probabilities in the wave packet calculations to any appreciable extent, as they occur for bond distances well beyond that found at the saddle point.

At H–H intramolecular distances $r \leqslant 4$ a_0, direct H_2–H_2 contacts in the (2×2) H_2 overlayer are negligible (see Fig. 2). Nevertheless, the H_2–Cu interaction obtained in this way may still differ from the interaction of isolated H_2 molecules with Cu. We will call the difference the through-lattice interaction. The absence of such an interaction has been verified through calculations employing a (3×2) coverage, where the H–H distance between H atoms of neighboring molecules is still only 9.6 a_0 for $r = 4.8$ a_0 (see Fig. 1). Results of calculations of the energy using a (3×2) coverage are compared with results of using a (2×2) coverage in Table IV. In each case the energy change per unit cell is calculated, with respect to a Cu slab and two free H atoms, upon approach of the H atoms to each other and to the Cu slab at the specified r and Z. We note that at $r \leqslant 4$ a_0 the differences in the energies are very small, but at $r = 4.8$ a_0 there is an additional 0.22 eV stabilization in the (2×2) case, equal to the one found in the bare overlayer calculation. It is then tempt-

FIG. 1. Plot illustrating different coverages of the (100) face of copper by periodic overlayers of H_2. In all cases, each molecule has its center of mass above a bridge site and its internuclear axis parallel to the surface, dissociating into neighboring hollow sites. The coverages illustrated are (a) the $\sqrt{2} \times \sqrt{2}$ coverage, (b) as (a), with the H atoms dissociated into the hollow sites ($r = 4.8$ a_0), (c) the 2×2 coverage, (d) as (c), with the H atoms dissociated into the hollow sites, and (e) the 3×2 coverage with the H atoms dissociated into the hollow sites.
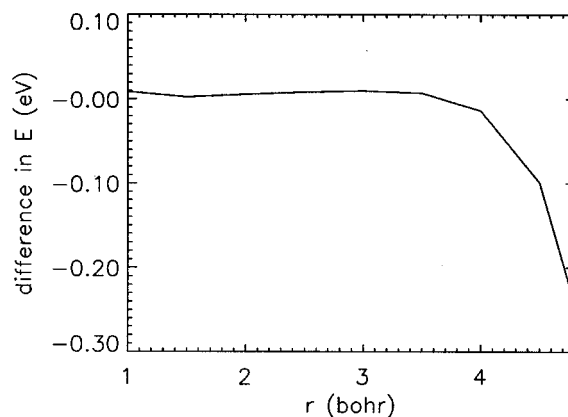
TABLE IV. The difference (in eV) between the potential energy of H$_2$ interacting with a copper slab (with respect to the Cu slab) as calculated for a 2×2 coverage and for a 2×3 coverage is given for a few points (r, Z) (in bohrs).

r	Z	Difference (2×2)–(3×2)
2.0	2.0	−0.04
4.0	2.0	−0.05
4.8	2.0	−0.22

TABLE VI. Properties of a (2×2) overlayer of hydrogen atoms adsorbed on the top, bridging, and hollow sites of two-layer copper slabs with the copper atoms in the bottom layer, a core up to $3p$ or up to $3d$. The first entry corresponds to the equilibrium bond distance (in bohrs), the second to the bond energy (in eV).

	Top	Bridging	Hollow
$3d$ core	2.91, −1.84	2.01, −2.43	1.17, −2.59
$3p$ core	2.88, −1.90	2.03, −2.49	1.19, −2.57

ing to conclude the stabilization to be due to direct H$_2$–H$_2$ interactions only, rather than to a through-lattice effect, but this would not be a valid statement: due to the way we have defined the through-lattice interaction, the concept is meaningful only in case the direct interactions between the H$_2$ molecules are negligible, which is not the case for the (2×2) coverage when $r = 4.8$ a_0.

The number of layers. To study the convergence with the number of layers of the copper slab we have calculated equilibrium distances and binding energies for hydrogen atoms adsorbed in a (2×2) overlayer on the top, bridging and hollow sites of a one-, two-, and three-layer copper slab. The copper atoms in the top layers have a frozen core up to $3p$, the copper atoms in the bottom layer a frozen core up to $3d$. Results are given in Table V. As can be seen, even in the worst case (hollow site atomic adsorption) the results of the two-layer calculation are already converged to within 0.07 eV compared to the three-layer results. This is similar to what was found before in calculations of chemisorption of CO on Cu(100), where the results of using four layers were found to be only marginally different from results using two layers (see Fig. 1 of Ref. 43). In the calculation of the potential energy surfaces, we therefore use a two-layer slab.

The slabs in the bottom layer have a frozen core up to $3d$ for economical reasons: the calculations are computationally less demanding. To show that this treatment of the lower layer of Cu atoms is justified, we compare in Table VI results of two calculations for the bond distance and bond energy of atomic hydrogen adsorbed in a (2×2) overlayer to a two-layer slab. In one calculation, the copper atoms in the bottom layer have a frozen core up to $3d$ as in the calculation of the PES's, in the other calculation a larger basis set of active orbitals is used (frozen core only up to $3p$). The results are given in Table VI. As can be seen, the results of using a frozen core up to $3d$ for the bottom layer atoms are converged to better than 0.06 eV for all sites. We conclude that using a $3d$ core for the copper atoms in the bottom layer is sufficient.

TABLE V. Properties of a (2×2) overlayer of hydrogen atoms adsorbed on the top, bridging, and hollow sites of a one-, two-, and three-layer copper slab. The first entry gives the molecule–surface equilibrium bond distance (in bohrs), the second entry the bond energy (in eV).

	Top	Bridging	Hollow
One	2.83, −1.48	1.81, −2.30	0.05, −1.85
Two	2.91, −1.84	2.01, −2.43	1.17, −2.59
Three	2.86, −1.89	1.99, −2.45	1.16, −2.52

Numerical integration. The accuracy of the numerical integration in real space, as measured by the deviation of numerical integrals from their known values, was 0.05%, the value of the "accint" parameter used in BAND being 3.5.[54] This gives an error in the calculated binding energies of about 0.01 eV. The irreducible wedge of the first Brillouin zone consists of two triangles. In each triangle six **k** points were chosen, allowing the use of the quadratic **k**-space integration method[58] in each triangle. The total number of **k** points is 9, of which 6 are symmetry unique. The error in the calculated binding energies caused by the numerical integration in **k** space is of the order of 0.03 eV, as determined from calculations using the values 3 and 5 for the "*k*-space" parameter in BAND.[54]

We conclude this section by remarking that based on the given convergence studies the PES's as calculated from the (2×2) hydrogen molecule overlayer adsorption to a two-layer copper slab should be near the density-functional limit results for values of $r \leq 4$ bohrs. We expect our results to be converged to within approximately 0.1 eV over the region of the PES important in calculating reaction probabilities using dynamics methods.

C. The LDA and GGA PES's for H$_2$+Cu(100)

To construct the 2-D LDA and GGA PES's, we have calculated energies of a (2×2) overlayer of H$_2$ molecules adsorbed to a two-layer Cu(100) slab for a number of values of z (the distance of the H$_2$ molecule to the top layer of the slab) and r (the internuclear distance in H$_2$). In each case, the energy reported is the energy per unit cell minus the energies of the Cu slab and two free H atoms. We used 5 values of z and 6 values of r, giving a total of 30 points. The calculations are for H$_2$ approaching with its internuclear axis parallel to the surface and dissociating over a bridge site into neighboring hollow sites. To locate the saddle point and obtain high accuracy of the fit in the region of the saddle point, the results of the calculations were fit, and the position of the saddle point was calculated from the fit. Next, we calculated the binding energy in 9 additional points distributed around the saddle point. These points were added to the set, giving the final PES's. The LDA and GGA PES's are shown in Fig. 3.

Clearly, the LDA PES shows no barrier to chemisorption: the hydrogen molecules dissociate smoothly into the hollow sites. The GGA PES shows a later barrier located at $r = 2.2$ bohrs and $Z = 1.9$ bohrs. The barrier height is 0.4 eV. Our LDA results are consistent with those recently obtained for the same system[19] and also for H$_2$+Cu(111) (Ref. 12) in
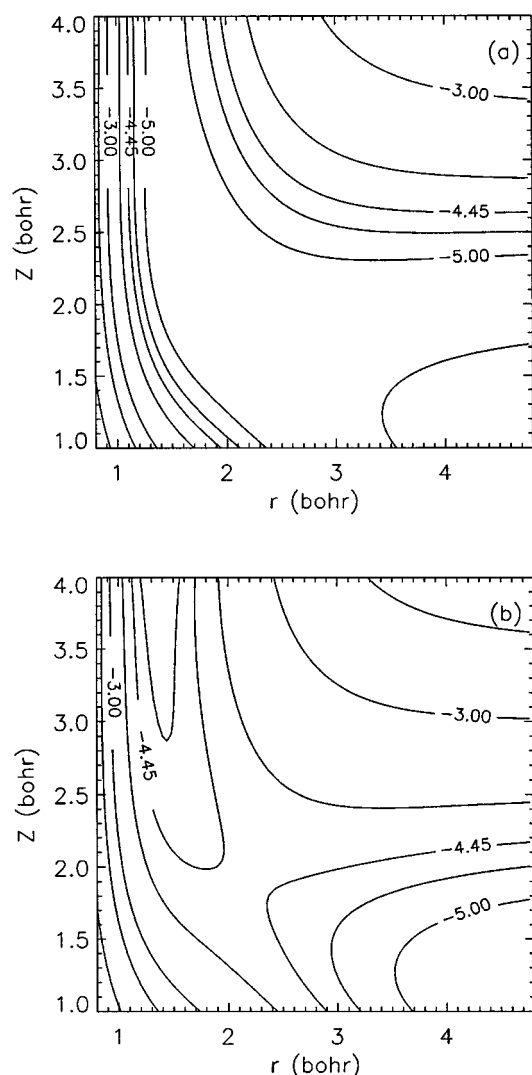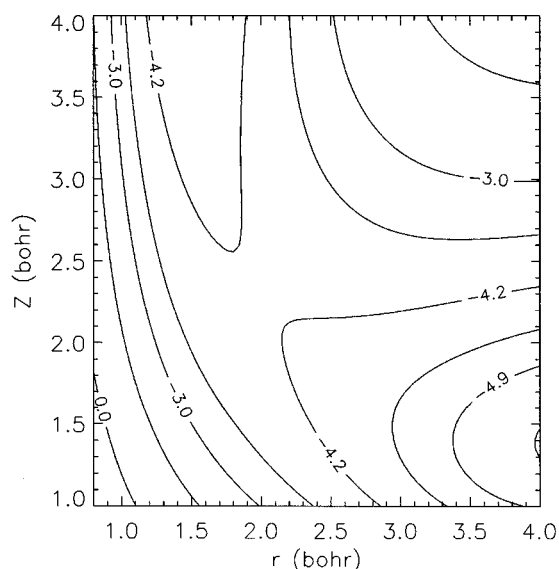
FIG. 4. Contour plot of the GGA potential energy surface as calculated using the same coverage of H₂ ($\sqrt{2}\times\sqrt{2}$) as used by White *et al.* (Ref. 19). The contours shown are for −4.9, −4.6, −4.18, −3.6, −3, −2, and 0 eV.

FIG. 3. Contour plots of the LDA (a) and GGA (b) potential energy surfaces. The contours shown are for −6, −5, −4.7, −4.44, −4, −3, −2, and 0 eV.

that they are qualitatively wrong: according to the LDA, either there is no barrier to dissociation or it is very small. Our GGA result for the barrier height is also consistent with the GGA result for H₂+Cu(111):[12] our barrier height for the more open (100) face is slightly smaller at 0.4 eV than that obtained for the more closed (111) face (0.5 eV), as would be expected. On the other hand, the barrier height we calculate is not consistent with the value of 0.9 eV calculated for the (100) face by White *et al.*[19] We are not entirely sure what is the cause of this discrepancy. Certainly, a barrier height of 0.9 eV seems too high when compared with the experimental results.[41] One reason for the discrepancy may be that White *et al.* have used a coverage that could be too high. With the $\sqrt{2}\times\sqrt{2}$ coverage they employ, the distance between H atoms of different H₂ molecules becomes $\sqrt{4.8^2+(4.8-r)^2}$ bohrs, compared to $(9.6-r)$ bohrs for the 2×2 coverage. At the saddle point ($r=2.2$ bohrs), this distance is considerably shorter for the $\sqrt{2}\times\sqrt{2}$ coverage (5.46 bohrs) than it is for the 2×2 coverage (7.4 bohrs). This suggests that direct H₂–H₂

interactions or through-lattice interactions may affect the calculation of the barrier height in case the higher coverage is used. To check this, we have also performed calculations employing a $\sqrt{2}\times\sqrt{2}$ coverage, otherwise using the same values for the other parameters (basis sets, number of layers, etc., see Sec. II B). The resulting PES is plotted in Fig. 4. The barrier height of this PES is 0.66 eV, which value is larger than that found for a 2×2 coverage by 0.26 eV, which explains at least part of the discrepancy (0.5 eV) found with the results of White *et al.*[19]

Another difference between the methods is that White *et al.* use pseudopotentials to model the core electrons of Cu where we use the frozen core approximation. In a sense the frozen core approximation may be said to be more robust, in that convergence with respect to the number of active atomic orbitals can easily be checked by decreasing the size of the frozen core. However, pseudopotentials can also give accurate results when chosen with care. Finally, White *et al.* use a slightly different GGA than we do. While we employ the gradient corrections of Becke[60] and Perdew,[61] the GGA used by White *et al.* is that due to Perdew and Wang.[62] This GGA has recently also been implemented in BAND, and calculations comparing results of using this GGA and using the GGA consisting of the Becke and Perdew corrections showed only small differences (less than 0.1 eV) in the total energies calculated for H₂+Cu. We conclude that it is not entirely clear why the difference between the barrier heights calculated by us and by White *et al.* should be so large. Roughly half of the difference can be explained by White *et al.* using a coverage that is too large. The discrepancy of our results clearly shows the need for performing comparisons of results of chemisorption calculations using different methods and codes.
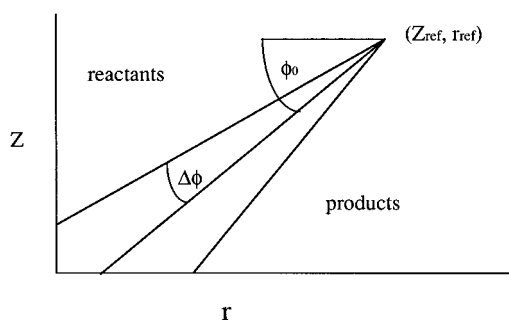
FIG. 5. Plot illustrating the division of coordinate space in reactants and products regions (see text).

TABLE VII. Fitting coefficients for the two-body part of the potential. For the meaning of the parameters, see the text.

Parameter	V^A	V^B
D_e (eV)	4.8286	2.597
x_e[a] (a_0)	1.40	1.18
a_1 (a_0^{-1})	2.282	1.190
a_2 (a_0^{-2})	1.555	0.583
a_3 (a_0^{-3})	0.753	0.113
a_4 (a_0^{-1})	2.23	1.20
a (eV)	24.0	45.81
b (a_0^{-1})	1.39	1.365

[a]x_e is r_e in the entrance channel (V^A) and Z_e in the exit channel (V^B).

III. FITTING THE POTENTIAL

Performing reaction dynamics on the density functional H₂+Cu(100) potential requires this potential to be known on a sufficiently dense grid of points. It is then desirable to have an analytical representation of this potential over a wide enough region of coordinate space, in the form of a fit. If we want to use the potential to calculate vibrational excitation probabilities and reaction probabilities, this fit should be accurate primarily in the entrance channel, the reaction region, and the part of the exit channel lying close to the reaction barrier. Our fitting strategy follows from these requirements. The fit consists of a two-body part and a three-body part. The two-body part yields quantitatively correct asymptotic behavior in the entrance channel (H₂+Cu), and qualitatively correct behavior in the exit channel and reaction zone. No attempt is made to model the r dependence of the potential in the exit channel for $r > 4.8$ a_0, where $r = 4.8$ a_0 corresponds to both H atoms being above the hollow site, the limit to which our potential extrapolates in the exit channel. At any rate, as was discussed in Sec. II B, the GGA potential is expected to be less accurate for $r > 4$ a_0. The fit is made accurate in the entrance channel, reaction zone, and start of the exit channel by fitting the three-body part. Actually, it is in the three-body part that we really fit the potential, whereas in the two-body part we only use information concerning the fragments and the general nature of the potential. As described below, for the three-body part we borrow a form used also in fitting potentials of triatomic molecules. The expression used has high flexibility, and should allow for higher accuracy than the much used London, Eyring, Polanyi, and Sato (LEPS) form,[64] which has fewer adjustable parameters.

In the two-body part of the potential, we use the now well established knowledge concerning the general features of the potential,[14] as others have done before,[33,35] and its asymptotic behavior. Briefly, the energy diagram for H₂+Cu(100) is divided into two regions by a seam, along which the saddle point or barrier to reaction is located. The seam is reasonably well described by a line lying in the (r,Z) plane, making an angle ϕ_0 with the r axis, and passing through the point (Z_{ref}, r_{ref}), (see also Fig. 5). Angles ϕ smaller than ϕ_0 correspond to the entrance channel, where H₂ is in its ground electronic state and has both an attractive interaction with the surface (the van der Waals interaction)

and a repulsive interaction (the Pauli repulsion). Thus, in the entrance channel (region A, reactants) the potential is given approximately by

$$V_{2b}^A(r,Z) = V_{att}(r) + V_{rep}(Z). \tag{1}$$

In writing Eq. (1), we neglect the van der Waals interaction for the moment. Angles ϕ larger than ϕ_0 correspond to the exit channel (region B, products), where H₂ behaves as if it is in an excited, repulsive electronic state, and the H atoms form chemical bonds to the surface

$$V_{2b}^B(r,Z) = 2V_{att}(Z) + V_{rep}(r). \tag{2}$$

To impose the proper asymptotic behavior on the potential in the entrance channel, the GGA bare H₂ potential was taken as $V_{att}(r)$ and fitted over the range $r = 0.75 - 3.0$ a_0 to a modified Rydberg form

$$V_{att} = -D_e \times [1.0 + a_1\rho + a_2\rho^2 + a_3\rho^3] \exp[-a_4\rho], \tag{3a}$$

where $\rho = r - r_e$. The constants obtained for the fit are collected in Table VII. The Pauli repulsion was taken as

$$V_{rep} = a \exp[-bZ], \tag{3b}$$

with the a and b constants taken from Ref. 13 (see also Table VII).

We proceed in a similar fashion in the exit channel. To obtain $V_{att}(Z)$, density functional (GGA) results for atomic hydrogen above the hollow site (see above) were fitted to the form of Eq. (3a) with $\rho = Z - Z_e$, where Z is in the range -0.5 to 3.0 a_0 (see Table VII for the coefficients thus obtained). The repulsive potential $V_{rep}(r)$ was taken as in Eq. (3b), with a and b fitted to an *ab initio* multiple reference double-excitation configuration-interaction (MRD-CI) potential[65] for the first excited state of H₂ [Z was replaced by r in Eq. (3b)].

Next we considered the potential given by $V(r,Z) = \min[V_{2b}^A(r,Z), V_{2b}^B(r,Z)]$. This potential is qualitatively similar to the full density functional potential, with the location of the seam given approximately by $\phi_0 = 61.5°$ and $Z_{ref} = 18.3$ a_0, for a preselected value of r_{ref} of 11.0 a_0. To now fit the full density functional potential, we start by producing a two-body potential V_{2b} which is somewhat smoother than the potential obtained by simply taking the minimum value of Eqs. (1) and (2). This is accomplished by defining a reaction region (region C, see also Fig. 5), given

TABLE VIII. Fitting coefficients for the three-body part of the potential. For the meaning of the parameters, see the text. Note that the point (r_0, Z_0) is *not* the saddle point.

Parameter	V^A	V^B
$\gamma_1 \ (a_0^{-1})$	1.0	1.15
$r_0 \ (a_0)$	1.89	1.89
$\gamma_2 \ (a_0^{-1})$	0.75	0.8
$Z_0 \ (a_0)$	2.08	2.08
c_0 (eV)	-1.9884	-2.1179
$c_1 \ (\text{eV} \ a_0^{-1})$	-3.4251	-4.0001
c_2	0.3355	0.2748
$c_{11} \ (\text{eV} \ a_0^{-2})$	-0.8331	-0.0385
c_{12}	-3.0379	-6.5386
c_{22}	0.4633	0.2111
$c_{111} \ (\text{eV} \ a_0^{-3})$	1.4237	1.8041
c_{112}	-5.1844	-1.8222
c_{122}	1.0940	-5.2617
c_{222}	-0.1435	0.4700
$c_{1111} \ (\text{eV} \ a_0^{-4})$	0.8313	-0.4233
c_{1112}	-2.1928	1.9003
c_{1122}	0.3939	-0.5171
c_{1222}	-0.2351	-2.7936
c_{2222}	-0.0075	-0.7040

by $\phi_0 - \Delta\phi \leq \phi \leq \phi_0 + \Delta\phi$ (we take $\Delta\phi = 2.5°$). The two-body potential is then obtained by switching smoothly from the entrance channel to the exit channel in region C

$$V_{2b} = V_{2b}^A(r,Z), \quad \phi < \phi_0 - \Delta\phi, \tag{4a}$$

$$V_{2b} = f_c(\phi) V_{2b}^A(r,Z) + [1 - f_c(\phi)] V_{2b}^B(r,Z),$$
$$\phi_0 - \Delta\phi \leq \phi \leq \phi_0 + \Delta\phi, \tag{4b}$$

$$V_{2b} = V_{2b}^B(r,Z), \quad \phi > \phi_0 + \Delta\phi, \tag{4c}$$

where the switching function is given by

$$f_c(\phi) = \tfrac{1}{2} + \tfrac{1}{2} \cos(\chi), \tag{5a}$$

$$\chi = \frac{[\phi - (\phi_0 - \Delta\phi)]\pi}{2\Delta\phi} \tag{5b}$$

and ϕ is defined by

$$\phi = \arctan \frac{(Z - Z_{\text{ref}})}{(r - r_{\text{ref}})}. \tag{5c}$$

The reason that Z_{ref} and r_{ref} were taken as large positive numbers is to allow the switching to be performed without singularities resulting in the energy-accessible coordinate region. The next step is where the actual fitting of the full density functional potential (GGA) is done. We obtain the density functional three-body potential by substracting V_{2b} from the full density functional potential. Next, in regions A and C the remaining term is fitted to a "three-body potential" of the form

$$V_{3b}^A(r,Z) = P(s_1, s_2)[1.0 - \tanh(\gamma_1 s_1)][1.0 - \tanh(\gamma_2 s_2)], \tag{6a}$$

$$P(s_1, s_2) = c_0 + c_1 s_1 + c_2 s_2 + c_{11} s_1^2 + c_{12} s_1 s_2 + \cdots \tag{6b}$$

retaining terms up to fourth order in Eq. (6b). In Eqs. (6), $s_1 = r - r_0$ and $s_2 = Z - Z_0$. For the coefficients obtained for

regions A and C, see Table VIII. The form of Eqs. (6) has been used successfully in fitting potentials of triatomic molecules.[66] It goes exponentially to zero for either r or Z (or both) large, while remaining finite for both r and Z small. In regions B and C the three-body GGA, potential is fitted to $V_{3b}^B(r,Z)$, which is identical in form to Eqs. (6) (see also Table VIII). A smooth fit of the three-body potential V_{3b} is then obtained by switching from $V_{3b}^A(r,Z)$ to $V_{3b}^B(r,Z)$ in region C using the same switching function [Eqs. (5)] as was used in producing a smooth two-body potential [Eqs. (4)]. The fit thus obtained deviated from the density functional potential values by less than 0.1 eV for total interaction energies smaller than -2.5 eV. Finally, in the product region the three-body potential V_{3b} is multiplied with the damping function f_d given by

$$f_d(Z) = \tfrac{1}{2} - \tfrac{1}{2} \cos(\alpha), \tag{7a}$$

$$\alpha = \frac{[z - (z_0 - \Delta z)]\pi}{2\Delta z}, \tag{7b}$$

with $z_0 = 0.8 \ a_0$ and $\Delta z = 0.2 \ a_0$. This only affects the full potential well into the product region, and should have no effect on the calculated reaction probabilities. The reason that we switch off the three-body potential in the product region for $Z < 1.0$ bohrs is that it does not perform well in extrapolating to values of Z smaller than 1 bohr, for which we have no GGA results. The fitted potential is plotted in Fig. 6.

IV. DYNAMICS CALCULATIONS

A. Method

The Hamiltonian describing the two-dimensional (2-D) dynamics of the H$_2$ molecule interacting with a rigid surface is
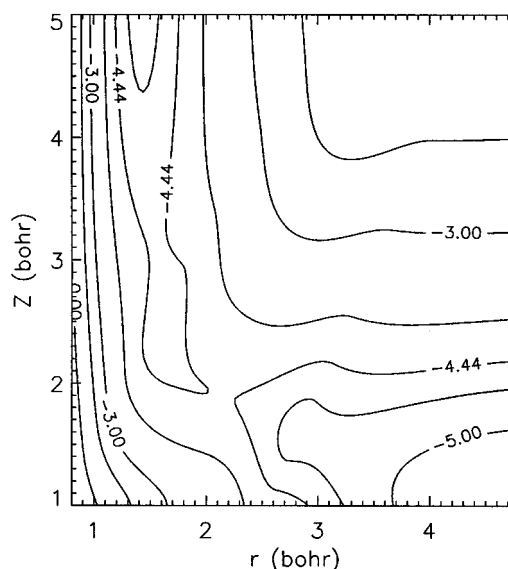

FIG. 6. Contour plot of the fit to the GGA potential energy surface. The contours shown are for -5, -4.7, -4.44, -4, -3, -2, and 0 eV.

$$\hat{H} = -\frac{1}{2M}\frac{\partial^2}{\partial Z^2} - \frac{1}{2\mu}\frac{\partial^2}{\partial r^2} + V(Z,r), \tag{8}$$

where Z is the distance from the surface to the molecular center of mass and r is the internuclear separation. The total mass and reduced mass are denoted by M and μ, respectively, and $V(Z,r)$ is the fit to the GGA potential energy of the H$_2$ molecule interacting with the rigid Cu(100) surface (see Sec. II C and Sec. III). Atomic units are used throughout unless otherwise stated. Since the Hamiltonian is independent of time, the formal solution to the time-dependent Schrödinger equation can be written as

$$\Psi(Z,r,t+\Delta t) = e^{-i\hat{H}\Delta t}\Psi(Z,r,t). \tag{9}$$

The wave function is propagated in time using the Chebyshev method.[67] This involves the evaluation of the action of the Hamiltonian on the wave function. The spatial derivatives occurring in the kinetic energy part of the Hamiltonian are evaluated using the Fourier method.[68,69] The evaluation of the action of the Hamiltonian is completed by multiplying the wave function at each grid point by the potential energy and adding the result to the kinetic energy contribution. The required computation times and memory requirements are reduced by representing the translational wave function on a two-dimensional L-shaped grid.[52] The grid is constructed so that it covers the reactants, interaction, and products regions of the potential energy surface. The amplitude of the wave function is negligible far outside these regions since the total energy of the molecule is much lower than the potential energy. In the L-shaped grid, 256 and 32 points were used in the Z coordinate in the interaction-reactants and products regions, respectively. In the r coordinate 16 and 48 grid points were used in the reactants and interaction-products regions, respectively. The grid covered the region from $Z=-1.0$ a_0 to $Z=37.25$ a_0 and from $r=0.0$ a_0 to $r=9.4$ a_0. An absorbing potential in the asymptotic region of the products channel was used to damp out the wave function and prevent reflection from the grid boundary. Its functional form is a power law potential[70]

$$V_{abs}(r) = \begin{cases} i\lambda[(r-r_0)/(r_{max}-r_0)]^2, & r \geq r_0 \\ 0, & r < r_0 \end{cases}, \tag{10}$$

with $r_0 = 4.8$ a_0 and $r_{max} = 9.4$ a_0, and $\lambda = 1.0$ eV. The transition probabilities were independent of small changes in these parameters.

Introduction of an absorbing potential results in an instability in the Chebyshev propagator when long propagation times are used.[71,72] For this reason, the time propagation was split up into smaller individual propagation steps each of which was 250 atomic time units long. The initial translational function at $t=0$ is written as the product of a vibrational eigenfunction for H$_2$ in r, χ_{v_0}, and a Gaussian in Z

$$\Psi(Z,r,t=0) = \chi_{v_0}(r)(2\pi\xi^2)^{-1/4}\exp\left[\frac{-(Z-Z_0)^2}{4\xi^2} + ik_0Z\right], \tag{11}$$

where Z_0 and k_0 are the average position and momentum, respectively, and ξ is the width of the wave packet. Values of $Z_0 = 17.0$ a_0 and $\xi = 1.118$ a_0 were used to define the initial
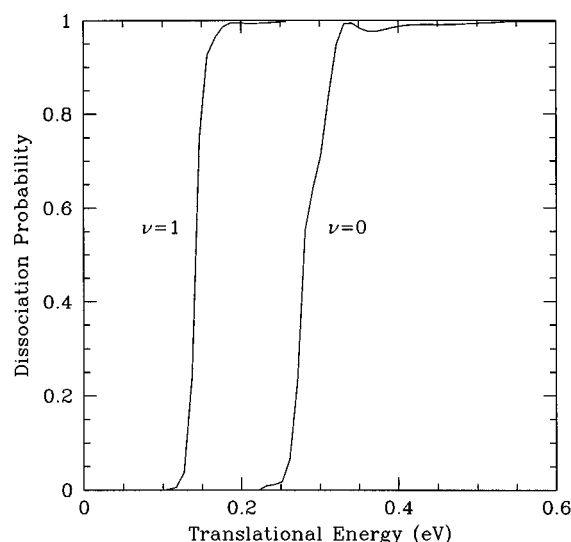

FIG. 7. The dissociation probability of H$_2$ is shown as a function of the collision energy for the ground and first excited vibrational states.

wave function. The H$_2$ vibrational eigenfunctions were calculated employing the discrete grid Hamiltonian method of Balint-Kurti *et al.*[73] and using the GGA H$_2$ potential as fitted to Eq. 3(a) (see also Table VII). After the interaction with the surface was complete and the scattered portion of the wave function reentered the asymptotic region of the reactants channel transition probabilities were calculated by determining the overlap of the final wave function with the asymptotic states of the system.[74,75] The dissociation probability at each energy was calculated by subtracting the sum of the probabilities for elastic and vibrationally inelastic scattering from unity.

Scattering information can be obtained over a wide range of energies from propagating a single wave function since the initial wave function has a broad momentum distribution. Calculations in which the $v=1$ channel was energetically open required longer propagation time and the number of grid points in the Z direction was doubled. Total propagation times varied from 18 000 to 26 000 atomic time units depending on the incident energy and the initial vibrational state. Variation of the grid parameters and propagation times showed that the calculated probabilities are converged. In evaluating the action of the Hamiltonian on the wave function, the interaction potential was cutoff at 3.0 and 6.0 eV for low and high incident energies, respectively.

B. Discussion

The dependence of the dissociation probability on the incident translational energy for $v_0=0$ and $v_0=1$ is shown in Fig. 7. For the ground vibrational state the dissociation probability increases rapidly for translational energies above 0.25 eV and reaches unity for energies of 0.33 eV and above. For the $v=1$ vibrationally excited state, dissociative adsorption becomes significant for translational energies exceeding 0.12 eV and saturates at approximately unity above 0.18 eV.

These results for the dependence of the adsorption probability on the kinetic energy can be well described by a functional form suggested by Harris[36]

$$P_v(E) = \tfrac{1}{2}[1 + \tanh\{(E - T(v))/W(v)\}],\qquad(12)$$

where T is the threshold energy (the value of the kinetic energy at which the dissociation probability is half the saturation value, which is 1 in the present case) and W is the width of dissociation probability versus energy curve, and both T and W are taken to be dependent on the initial vibrational state v of the molecule. The values we calculate are $T(0) = 0.28$ eV, $T(1)$ is 0.14 eV, $W(0) = 0.03$ eV, and $W(1) = 0.01$ eV. Our calculations show only little vibrationally inelastic scattering from the $v = 0$ state to the $v = 1$ state, the vibrational excitation probability reaching a maximum at 0.002 for $E = 0.74$ eV.

Experimental dissociation probabilities are available from the molecular beam work of Anger *et al.*[1] Their results show the onset of sticking to lie at a translational energy of approximately 0.2 eV, the sticking coefficient rising to approximately 0.05 at $E = 0.45$ eV. For higher collision energies no results are available. Theoretical work[33,36] indicated that initially vibrationally excited H$_2$ dissociates at lower collision energies than vibrationless H$_2$: the stretching of the bond in the vibrationally excited molecule helps to overcome the reaction barrier which is "late," i.e., placed in the exit channel where the molecular bond is stretched. The theoretical findings were in agreement with the results of seeded beam experiments on H$_2$+Cu(110),[5,6] which showed higher dissociation probabilities at similar collision energies for vibrationally hotter beams. Originally, Anger *et al.*[1] found no evidence in their experiments for vibrational enhancement of dissociation. However, in a careful analysis of their experiments Michelsen and Auerbach[41] found subtle deviations from normal energy scaling, which were well explained if a lower threshold for dissociation were assumed for $v = 1$ H$_2$ than for $v = 0$ H$_2$. Their analysis puts the $v = 1$ threshold at 0.26 eV and the $v = 0$ threshold at approximately 0.55 eV. Also, over the range of energies used in the experiment of Anger *et al.*, most of the observed sticking should be due to the vibrationally excited H$_2$ present in the beam. The idea that initial vibrational excitation enhances dissociation has been confirmed by recent experiments which measure the kinetic energies of desorbing H$_2$ in a state-selective manner.[8]

Comparing our results for the thresholds with the results of the analysis by Michelsen and Auerbach,[41] we find that our 2-D results for the thresholds are too low, the $v = 1$ threshold (0.14) by approximately 0.1 eV and our $v = 0$ threshold by approximately 0.3 eV. However, it is known from comparisons of 2-D computational results with results of higher dimensionality calculations[27,38,53] that the 2-D thresholds are usually too low. The 2-D potential energy surface used in our calculation is for an orientation and point of impact of H$_2$ which are optimal (or near optimal) in the sense that the barrier to dissociation is at its lowest value. Calculations of higher dimensionality sample a distribution of barrier heights, which should push up the threshold by averaging. Previous calculations on H$_2$+Cu(110) (Ref. 27) found an increase of the $v = 0$ threshold by 0.2 eV when going

from two dimensions to six dimensions (the 6-D calculations were done using the quasiclassical method). Whether we will see a similar or even higher increase for the $v = 0$ threshold, and whether our $v = 1$ threshold will go up by less in future higher dimensionality calculations remains to be seen. Nevertheless, at this point we find it encouraging that the thresholds we obtain using our potential energy surface are close to the experimental values, knowing also that calculations of higher dimensionality should move them further in the right direction.

Experiments[7,10] on D$_2$ and H$_2$+Cu(111) find high probabilities for vibrational excitation of the molecule from the $v = 0$ state to the $v = 1$ state (for D$_2$, a value in the range 0.3–0.4 was reported for a collision energy of approximately 0.8 eV in both experiments). As far as we know, no experimental results are available for the (100) face at present. Our calculations find vibrational excitation probabilities which are lower by two orders of magnitude at similar collision energies. It is intriguing that calculations employing a model potential energy surface for H$_2$+Cu(100) (Ref. 34, see Table I thereof) similarly find low excitation probabilities, while calculations[21,24] employing a model potential energy surface for H$_2$+Cu(111) find vibrational excitation probabilities of the same order as the experiments for this system. Recent theoretical work[40] cautions that calculations of higher dimensionality are required for obtaining accurate values for dissociation thresholds and vibrational excitation thresholds simultaneously. Nevertheless, an interesting question that emerges is whether vibrationally inelastic scattering is much more efficient on the (111) face than on the (100) face. Hopefully, experiments on the (100) face will address this question in the near future.

V. CONCLUSIONS

We have used density functional theory (DFT) to calculate 2-D potential energy surfaces (PES's) for dissociative chemisorption of H$_2$ on the (100) face of copper. The PES's are for H$_2$ approaching with its internuclear axis kept parallel to the surface and dissociation over a bridge site into hollow sites. While one PES was computed within the local density approximation (LDA), the Becke and Perdew nonlocal or gradient corrections to the exchange-correlation energy were added in the calculation of the other surface (GGA).

Our DFT results are fully consistent with the results recently obtained by Hammer *et al.*[12] for H$_2$+Cu(111). In particular, the LDA surface shows no barrier to chemisorption, which is a qualitatively wrong result. On the other hand, a late type barrier of 0.4 eV is found for the GGA surface. This is somewhat smaller than the barrier found[12] for the less open (111) surface, as would be expected. The calculated barrier height is also consistent with the experimentally determined thresholds for dissociation of H$_2$. On the other hand, our (GGA) result for the barrier height is not consistent with the value calculated for H$_2$+Cu(100) by White *et al.*[19] However, their value (0.9 eV) seems to be too high compared with both experiment and the barrier value calculated for the (111) face.[12] It is quite likely that the H$_2$ coverage employed in their calculations was too high. Using the same coverage as employed by White *et al.* (the $\sqrt{2} \times \sqrt{2}$ coverage)

moves our calculated barrier height up by 0.26 eV. Furthermore, White *et al.* used pseudopotentials to model the interaction of the valence electrons with the core electrons. In our work, this interaction is modeled using the frozen core approximation, which is more robust at least in the sense that convergence of total energy results with the size of the frozen core can be easily checked. The discrepancy of our results and those of White *et al.* show the need for performing comparisons of different methods and codes for calculating chemisorption energies within a DFT/slab approach.

Borrowing an expression used to fit PES's for triatomics and using a switching function to describe the transition from the reactants channel to the products channel, a fit was made of the (GGA) PES. The method used allowed an accuracy of better than 0.1 eV in the entire region accessible in collisions with translational energies less than 2 eV. The fit was subsequently used to calculate reaction thresholds for H_2 in its $v=0$ and $v=1$ initial vibrational states. While our 2-D values for the $v=0$ and $v=1$ thresholds are not in full agreement with experiment, the deviations are in the right direction, in that the calculated thresholds are too small, by 0.1 eV for $v=1$ and 0.3 eV for $v=0$. Calculations of higher dimensionality should sample a distribution of (higher) barriers, and should result in better agreement with experiment. Our present results give us some confidence in the accuracy of the calculated GGA PES. We hope to be able to pass a more definite judgment on the quality of our DFT calculations in the near future, by calculating a full 6-D PES, and subsequently performing dynamics calculations on that surface.

ACKNOWLEDGMENTS

[1] G. Anger, A. Winkler, and K. D. Rendulic, Surf. Sci. **220**, 1 (1989).

[2] D. J. Auerbach, C. T. Rettner, and H. A. Michelsen, Surf. Sci. **283**, 1 (1993).

[3] M. Balooch, M. J. Cardillo, D. R. Miller, and R. E. Stickney, Surf. Sci. **46**, 358 (1974).

[4] H. F. Berger, M. Leisch, A. Winkler, and K. D. Rendulic, Chem. Phys. Lett. **175**, 425 (1990).

[5] B. E. Hayden and C. L. A. Lamont, Phys. Rev. Lett. **63**, 1823 (1989).

[6] B. E. Hayden and C. L. A. Lamont, Surf. Sci. **243**, 31 (1991).

[7] A. Hodgson, J. Moryl, P. Traversaro, and H. Zhao, Nature **356**, 501 (1992).

[8] H. A. Michelsen, C. T. Rettner, D. J. Auerbach, and R. N. Zare, J. Chem. Phys. **98**, 8294 (1993).

[9] P. B. Rasmussen, P. M. Holmblad, H. Christoffersen, P. A. Taylor, and I. Chorkendorff, Surf. Sci. **287–288**, 79 (1993).

[10] C. T. Rettner, D. J. Auerbach, and H. A. Michelsen, Phys. Rev. Lett. **68**, 2547 (1992).

[11] C. T. Rettner, D. J. Auerbach, and H. A. Michelsen, Phys. Rev. Lett. **68**, 1164 (1992).

[12] B. Hammer, M. Scheffler, K. W. Jacobsen, and J. K. Nørskov, Phys. Rev. Lett. **73**, 1400 (1994).

[13] J. Harris and A. Liebsch, Phys. Scr. T **4**, 14 (1983).

[14] J. Harris and S. Anderson, Phys. Rev. Lett. **55**, 1583 (1985).

[15] J. Harris, S. Andersson, C. Holmberg, and P. Nordlander, Phys. Scr. T **13**, 155 (1986).

[16] J. E. Müller, Surf. Sci. **272**, 45 (1992).

[17] J. K. Nørskov, J. Chem. Phys. **90**, 7461 (1989).

[18] J. A. White and D. M. Bird, Chem. Phys. Lett. **213**, 422 (1993).

[19] J. A. White, D. M. Bird, M. C. Payne, and I. Stich, Phys. Rev. Lett. **73**, 1404 (1994).

[20] J. Dai, J. Sheng, and J. Z. H. Zhang, J. Chem. Phys. **101**, 1555 (1994).

[21] G. R. Darling and S. Holloway, J. Chem. Phys. **97**, 734 (1992).

[22] G. R. Darling and S. Holloway, Chem. Phys. Lett. **191**, 396 (1992).

[23] G. R. Darling and S. Holloway, J. Chem. Phys. **97**, 5182 (1992).

[24] G. R. Darling and S. Holloway, Surf. Sci. **307–309**, 153 (1994).

[25] G. R. Darling and S. Holloway, Surf. Sci. **304**, L461 (1994).

[26] C. Engdahl, B. I. Lundqvist, U. Nielsen, and J. K. Nørskov, Phys. Rev. B **45**, 11362 (1992).

[27] C. Engdahl and U. Nielsen, J. Chem. Phys. **98**, 4223 (1993).

[28] C. Engdahl and B. I. Lundqvist, Chem. Phys. Lett. **215**, 103 (1993).

[29] A. Gross, Surf. Sci. **314**, L843 (1994).

[30] A. Grüneich, A. J. Cruz, and B. Jackson, J. Chem. Phys. **98**, 5800 (1993).

[31] D. Halstead and S. Holloway, J. Chem. Phys. **88**, 7197 (1988).

[32] D. Halstead and S. Holloway, J. Chem. Phys. **93**, 2859 (1990).

[33] M. R. Hand and S. Holloway, J. Chem. Phys. **91**, 7209 (1989).

[34] M. Hand and S. Holloway, Surf. Sci. **211–212**, 940 (1989).

[35] J. Harris, S. Holloway, T. S. Rahman, and K. Yang, J. Chem. Phys. **89**, 4427 (1988).

[36] J. Harris, Surf. Sci. **221**, 335 (1989).

[37] S. Küchenhoff and W. Brenig, Surf. Sci. **258**, 302 (1991).

[38] U. Nielsen, D. Halstead, S. Holloway, and J. K. Nørskov, J. Chem. Phys. **93**, 2879 (1990).

[39] J. Sheng and J. Z. H. Zhang, J. Chem. Phys. **99**, 1373 (1993).

[40] G. R. Darling and S. Holloway, J. Chem. Phys. **101**, 3268 (1994).

[41] H. A. Michelsen and D. J. Auerbach, J. Chem. Phys. **94**, 7502 (1991).

[42] B. Hammer, K. W. Jacobsen, and J. K. Norskov, Phys. Rev. Lett. **70**, 3971 (1993).

[43] P. H. T. Philipsen, G. te Velde, and E. J. Baerends, Chem. Phys. Lett. **226**, 583 (1994).

[44] E. Folga and T. Ziegler, J. Am. Chem. Soc. **115**, 5169 (1993).

[45] A. D. Becke, Int. J. Quantum Chem. S **23**, 599 (1989).

[46] A. D. Becke, J. Chem. Phys. **96**, 2155 (1992).

[47] B. G. Johnson, P. M. W. Gill, and J. A. Pople, J. Chem. Phys. **98**, 5612 (1993).

[48] T. Ziegler, Chem. Rev. **91**, 651 (1991).

[49] B. Hammer, K. W. Jacobsen, and J. K. Nørskov, Phys. Rev. Lett. **69**, 1971 (1992).

[50] G. te Velde and E. J. Baerends, Chem. Phys. **177**, 399 (1993).

[51] D. Post and E. J. Baerends, J. Chem. Phys. **78**, 5663 (1983).

[52] R. C. Mowrey, J. Chem. Phys. **94**, 7098 (1991).

[53] A. J. Cruz and B. Jackson, J. Chem. Phys. **94**, 5715 (1991).

[54] G. te Velde and E. J. Baerends, Phys. Rev. B **44**, 7888 (1991).

[55] P. Hohenberg and W. Kohn, Phys. Rev. B **136**, 864 (1964).

[56] W. Kohn and L. J. Sham, Phys. Rev. A **140**, 1133 (1965).

[57] G. te Velde and E. J. Baerends, J. Comput. Phys. **99**, 84 (1992).

[58] G. Wiesenekker, G. te Velde, and E. J. Baerends, J. Phys. C **21**, 4263 (1988).

[59] S. H. Vosko, L. Wilk, and M. Nusair, Can. J. Phys. **58**, 1200 (1980).

[60] A. D. Becke, Phys. Rev. A **38**, 3098 (1988).

[61] J. P. Perdew, Phys. Rev. B **33**, 8822 (1986).

[62] J. P. Perdew, J. A. Chevary, S. H. Vosko, K. A. Jackson, M. R. Pederson, D. J. Singh, and C. Fiolhais, Phys. Rev. B **46**, 6671 (1992).

[63] A. D. Becke, in *The Challenge of f and d Electrons*, edited by D. R. Salahub and M. C. Zerner (American Chemical Society, Washington, DC, 1989), p. 165.

[64] A. E. Depristo and A. Kara, Adv. Chem. Phys. **77**, 163 (1991).

[65] M. C. van Hemert (private communication).

[66] K. S. Sorbie and J. N. Murrell, Mol. Phys. **29**, 1387 (1975).

[67] H. Tal-Ezer and R. Kosloff, J. Chem. Phys. **81**, 3967 (1984).

[68] M. D. Feit, J. A. Fleck, and A. Steiger, J. Comput. Phys. **47**, 412 (1982).

[69] D. Kosloff and R. Kosloff, J. Comput. Phys. **52**, 35 (1983).

[70] T. Seideman and W. H. Miller, J. Chem. Phys. **96**, 4412 (1992).

[71] R. C. Mowrey, J. Chem. Phys. **99**, 7049 (1993).

[72] D. Neuhauser, M. Baer, R. S. Judson, and D. J. Kouri, Comput. Phys. Commun. **63**, 460 (1991).

[73] C. C. Marston and G. G. Balint-Kurti, J. Chem. Phys. **91**, 3571 (1989).

[74] R. C. Mowrey and D. J. Kouri, J. Chem. Phys. **84**, 6466 (1986).

[75] R. C. Mowrey and D. J. Kouri, J. Chem. Phys. **86**, 6140 (1987).